ACS OMEGA

http://pubs.acs.org/journal/acsodf

Article

Optical Anion Receptors with Urea/Thiourea Subunits on a TentaGel Support

Bruno Zavala-Contreras, Hisila Santacruz-Ortega,* Angel Ulises Orozco-Valencia, Motomichi Inoue, Karen Ochoa Lara, and Rosa-Elena Navarro

Cite This: *ACS Omega* 2021, 6, 9381−9390

Read Online

ACCESS | Metrics & More | Article Recommendations | Supporting Information

ABSTRACT: Two simple chemosensors with urea (L1) and thiourea (L2) groups were synthesized and studied by different spectroscopic techniques. Both receptors can sense acetate (Ac^-), dihydrogen phosphate ($H_2PO_4^-$), and fluoride (F^-) anions, accompanied by changes in UV−vis and ^1H NMR spectra, and an optical response is observed as a color change of the solutions due to deprotonation and hydrogen-bonding processes. Also, L1 and L2 were supported on TentaGel resins (R1 and R2), and their fluoride-sensing properties in DMSO and water solutions were studied. Interestingly, R2 can sense fluoride ions in sample solutions of 100% water.

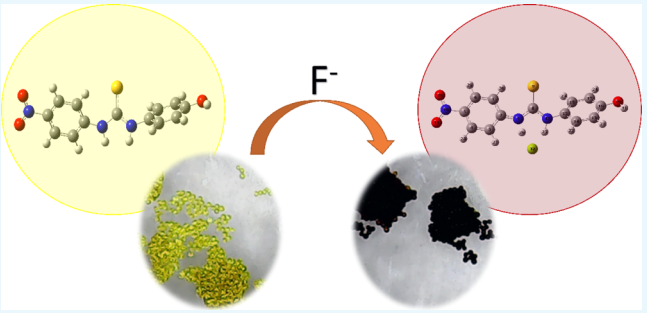

INTRODUCTION

In the past few years, work has been carried out to discover and improve analytical methods for a trustful sensing and detection of different species.[1] The detection, differentiation, and visualization of compounds as gases, liquids, and ions are important challenges for the design of optically selective chemosensors.[2] Real-time monitoring of the concentration of anions in aqueous solution and the qualitative determination in a wide range of concentrations are important in environmental and health issues as well as scientific and industrial applications.[3,4]

Among the techniques used for anion detection are electrochemical analysis, ion-selective electrode, and NMR.[5] However, these techniques present disadvantages as they use expensive instruments and require time-consuming and careful manipulation of well-trained technicians. Because of these disadvantages, colorimetric and fluorescent molecules are attractive for the design and study of new simple chemosensors capable of detecting species as anions as they could show great sensibility with detection limits of subparts per million.[6,7]

There are a big number of optical sensors that have been developed for anion detection. The used methods for the sensors depend on strong receptor−anion interactions, like acid−base interactions, electrostatic interactions, and hydrogen bonds, among others.[8−10]

Anion colorimetric sensors in which hydrogen bonding is involved have been designed and studied for many years.[11] Among these sensors are the ones using aromatic rings along with urea and thiourea groups as their NH units act as hydrogen-bond donors to bind to anions and cause a change in the chromogenic properties of the receptor. This can be translated as a color change of solution that can be perceived by the naked eye when anions are present.[12−14]

Some of the challenges to overcome for this kind of chemosensors are solubility and competition with the solvent: the most commonly used are polar aprotic solvents, like dimethyl sulfoxide (DMSO), which make the study of real samples difficult in aqueous solution and biological samples.[13]

One of the strategies used to solve these problems is to support anion receptors in different materials like Tentagel resins.[15] These copolymers, which consist of a polystyrene (PS) and polyethylene glycol (PEG), can be swelled in almost all solvents due to PEG so that the hydrophilic and hydrophobic properties are given to the resin.[16,17]

Herein, we describe the development of two simple urea and thiourea anion receptors (L1 and L2, respectively) containing a phenol and nitrophenyl rings as chromogenic groups. We investigated their anion-sensing properties toward acetate, phosphate, and fluoride anions in DMSO solution through different spectroscopic techniques. TentaGel HL-Br resin was chosen as a solid support, to which the receptors were linked by the reaction of their phenol group with the functional Br group of the resin. The functionalized resins were studied in aqueous and DMSO solutions for proving the fluoride-sensing capacity.

Received: November 13, 2020
Accepted: March 17, 2021
Published: March 31, 2021

https://doi.org/10.1021/acsomega.0c05554
ACS Omega 2021, 6, 9381−9390

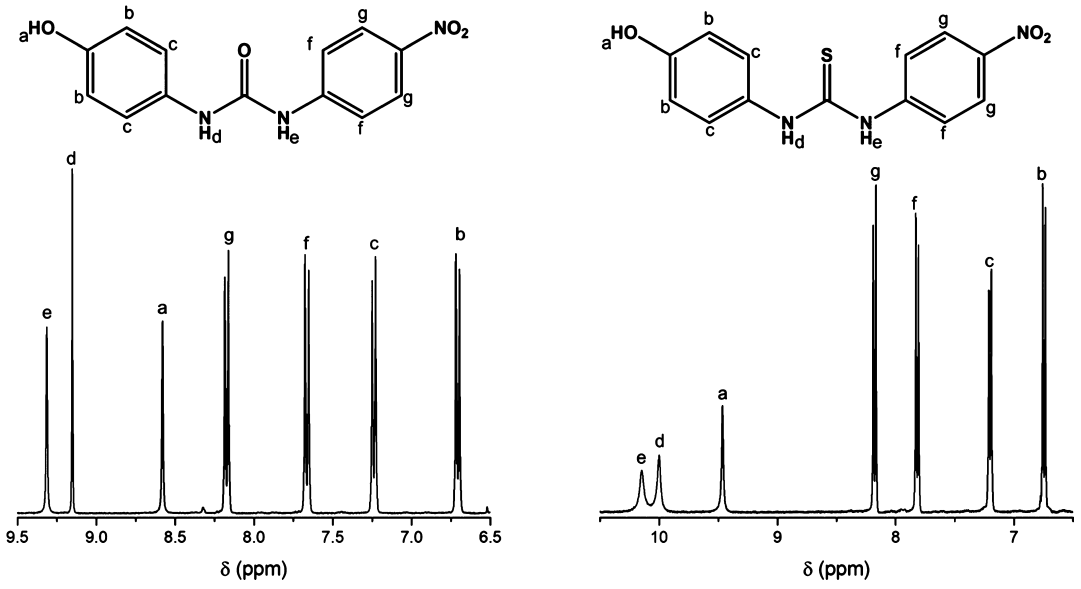

Figure 1. Receptors L1 (left) and L2 (right) and their ^{1}H NMR signal assignments.

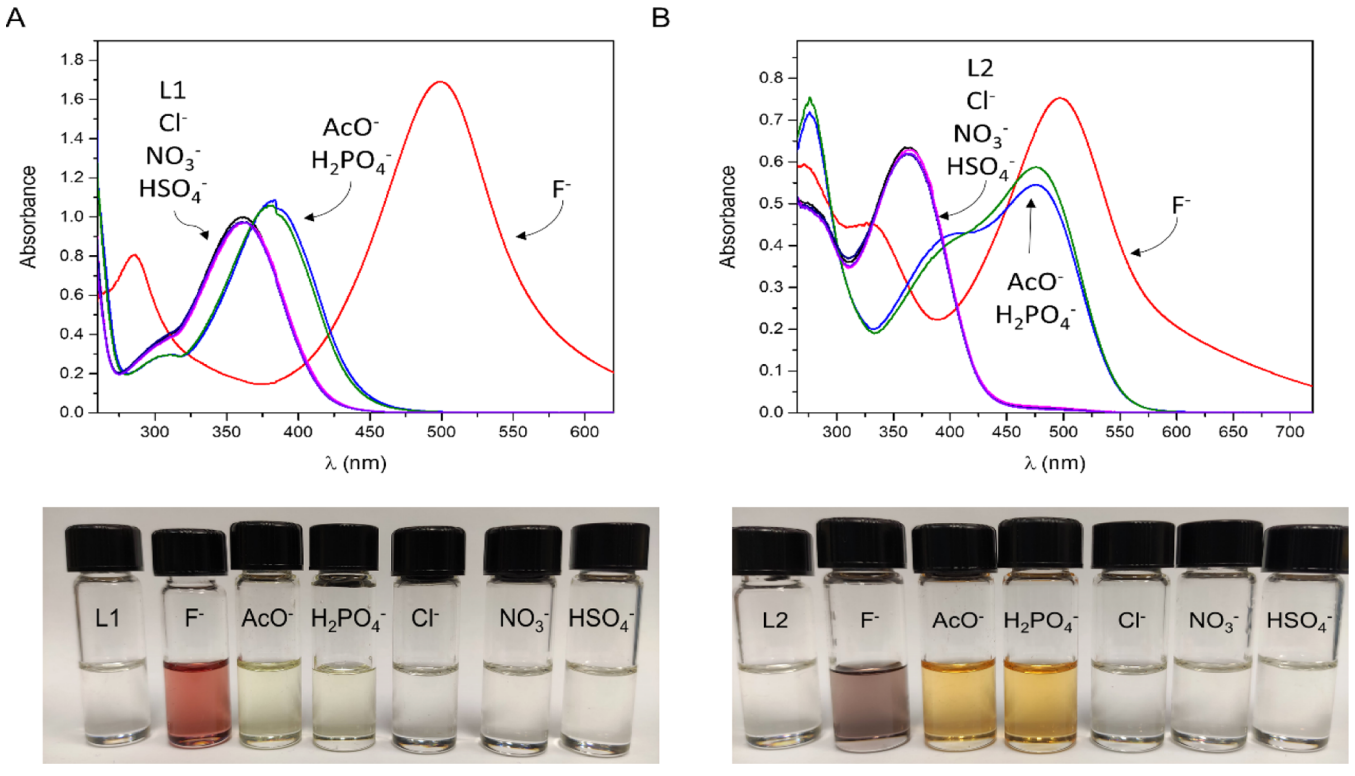

Figure 2. Absorbance and color changes of L1 (A) and L2 (B) (5×10^{-5} M) treated with an excess of different guest anions (F^-, AcO^-, Cl^-, and $H_2PO_4^-$).

RESULTS AND DISCUSSION

The receptors were synthesized in a single step, by the reaction of *p*-aminophenol with *p*-nitrophenyl isocyanate (L1) or *p*-nitrophenyl thiocyanate (L2) (Figure 1). The receptors were obtained in quantitative yields, and their purity was verified by different techniques such as melting joint, FT-IR, ^{1}H NMR, ^{13}C NMR, UV−vis, and mass spectrometry. The data are presented in the Experimental Section.

Reactivity of Receptors toward Anions. Both receptors L1 and L2 were dissolved in DMSO during UV−vis experiments. The UV−vis spectrum of the free receptor L1 exhibited two $\pi \rightarrow \pi^*$ absorption bands with maxima at 300 and 361 nm (for aromatic ring with NO_2). These transitions were observed at 274 and 372 nm, respectively, for L2. The anion-binding ability of L1 and L2 toward the anions Cl^-, $H_2PO_4^-$, AcO^-, HSO_4^-, NO_3^-, and F^- was investigated through colorimetric analysis in DMSO.

Figure 2 shows the UV−vis spectra of L1 and L2 receptors in the presence of the different anions studied, along with the photographs of the solutions. In the case of L1, a change in color was observed when F^- was added to the receptor solution: the UV band showed a bathochromic shift (361−382

https://doi.org/10.1021/acsomega.0c05554
ACS Omega 2021, 6, 9381−9390

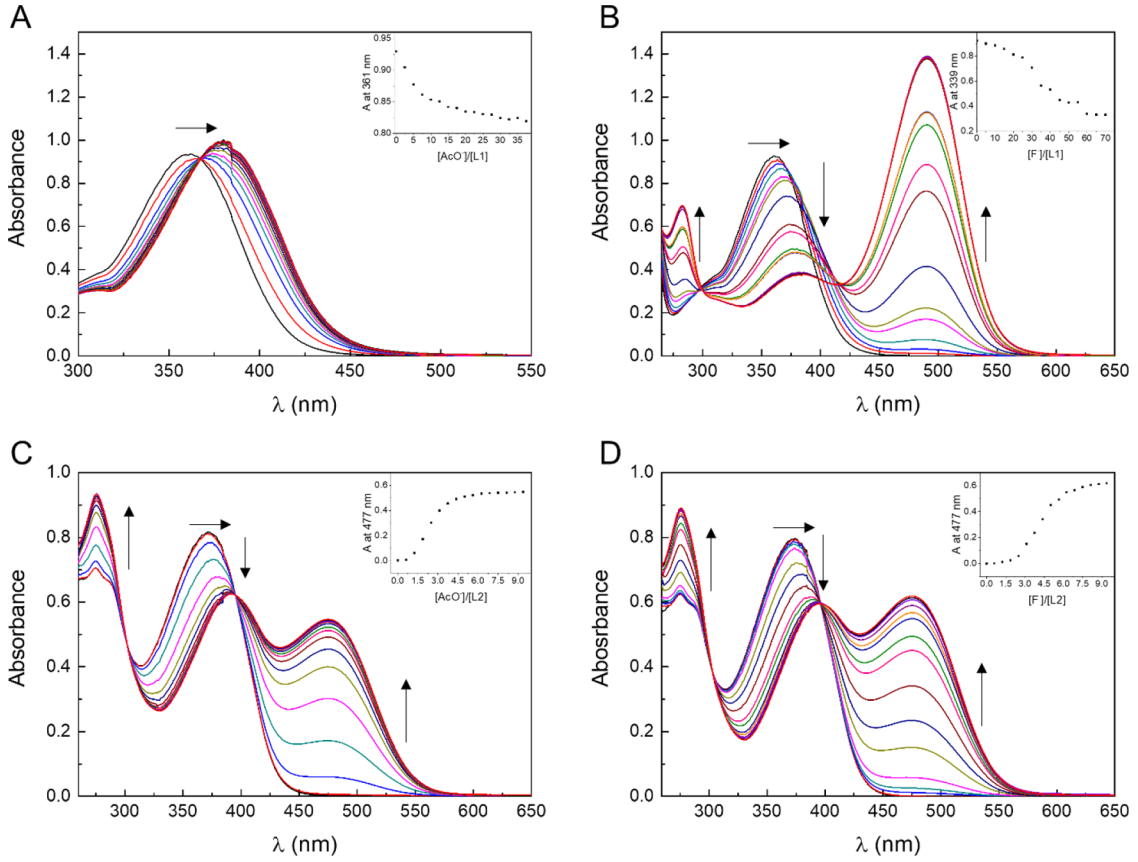

Figure 3. UV−vis titration in DMSO of (A) L1 (5×10^{-5} M) with TBA acetate (0.075 M). (B) L1 (5×10^{-5} M) with TBA fluoride (0.15 M). (C) L2 (5×10^{-5} M) with TBA acetate (0.018 M). (D) L2 (5×10^{-5} M) with TBA fluoride (0.018 M).

nm) and hypochromic effect, and a new band appeared at 499 nm, resulting in a change in color of the solution from pale yellow to red. When AcO^- and $H_2PO_4^-$ anions were added to L1 solution, a bathochromic shift occurred (361−382 nm), and the hyperchromic effect was observed only in the case of AcO^-.

For the other studied receptor L2, the presence of Cl^-, NO_3^-, and HSO_4^- ions did not cause any change in the spectrum (Figure 2). The presence of F^-, AcO^-, and $H_2PO_4^-$ ions caused a bathochromic shift in addition to the appearance of a new band at 497 and 477 nm, respectively, accompanying a color change from pale yellow to purple in the case of F^- and to bright yellow in the case of AcO^- and $H_2PO_4^-$. In order to study these changes in detail, UV−vis and ^1H NMR titrations, as well as Fourier transform infrared (FT-IR) and theoretical computer studies, were carried out.

UV−Vis Titrations of L1 and L2 toward Anions in DMSO. Titrations of solutions of L1 and L2 were carried out by adding tetrabutylammonium (TBA) salts of F^-, AcO^-, and $H_2PO_4^-$ in DMSO. Figure 3B shows that the titration of L1 (5×10^{-5} M) with F^- (0.15 M) exhibited a red shift of the absorption band (361−382 nm) as the anion concentration was increased. In addition, a new absorption band appeared at 490 nm due to charge transfer caused by the deprotonation of the NH groups of the receptor L1; this behavior is responsible for the color change of solution.

Titration of L1 (5×10^{-5} M) with AcO^- (Figure 3A) and $H_2PO_4^-$ (Figure S4 in Supporting Information) showed a similar red shift from 361 to 380 and 375 nm, respectively, with increasing the anion concentration in the solution. However, no new absorption band appeared at a longer wavelength; this fact suggests that the type of interaction of L1 with AcO^- and $H_2PO_4^-$ is hydrogen bonding. L1 showed higher sensibility toward AcO^- (Figure 3A) and H_2PO_4 because of their geometry[18] as the titrations were performed at a lower concentration of these anions (0.075 M).

Titrations of L2 (5×10^{-5} M) with F^- (Figure 3D), AcO^- (0.018 M) (Figure 3C), and $H_2PO_4^-$ (Figure S5) showed a bathochromic shift (372 to 396, 390, and 375 nm, respectively) and a decrease in the absorbance band. Likewise, a new charge-transfer absorption band appeared at 497 with F^- and 477 nm with AcO^- and $H_2PO_4^-$ anions, indicating that the protons in the thiourea NH groups are more acidic than in the urea NH groups (L1).[19−21] Titrations of L1 and L2 with F^-, and L2 with AcO^- show a sigmoidal curve, differing from that predicted for ordinary 1:1-complexation. This observation suggests a positive cooperative binding process due to the presence of more than one binding site in the receptors L1 and L2. From the absorption titration plot, the binding schemes were interpreted by using an interactive data fitting procedure on the basis of eq 1, in which a compound L is in equilibrium between two states denoted by La and Lb

$$K_{ism} = [Lb]/[La] \text{ for La} \rightleftharpoons \text{Lb} \quad (1)$$

When a compound (or a receptor) L takes two states La and Lb that have different interactions with a guest ion at the same time in the same conditions (like conformational isomerism, tautomerism, and protonation equilibrium), the equilibrium is controlled by a single constant.

https://doi.org/10.1021/acsomega.0c05554
ACS Omega 2021, 6, 9381−9390

Table 1. Formation Constant (K/M^{-1}) Determinate in Solution (DMSO) by UV−vis; the Asterisked Values are K_{ism}

	K		
receptor	F	Ac^-	$H_2PO_4^-$
L1	3.59 × 103 ± 3.00%*	3.66 × 103 ± 0.39%	2.54 × 103 ± 0.34%
L2	2.26 × 104 ± 1.06%*	2.79 × 104 ± 1.08%*	3.20 × 103 ± 0.29%

The equilibrium depends on the environmental conditions such as electrolyte and solvent effects. When the equilibrium is displaced by an anion effect, the stimulation is most reasonably expressed by the logistic function, and the concentrations of the two species are formulated as follows

$$[La] = [L]_t/\{1 + \exp[w(C_{eq} - [S])]\} \quad (2)$$

$$[Lb] = [L]_t \exp[w(C_{eq} - [S])]/\{1 + \exp[w(C_{eq} - [S])]\} \quad (3)$$

Here, $[L]_t$ is the total concentration, $[S]$ is the concentration of simulant (such as F^- or AcO^-), C_{eq} is the concentration at equivalent point or $[S]$ at $[La] = [Lb]$, and w is the width of response. The resulting spectral change is given by a weighted average of the intrinsic spectral intensities I_a of La and I_b of Lb at $[L]_t$.

$$I = (I_a[La] + I_b[Lb])/[L]_t \quad (4)$$

The curve fitting is performed for variables w and C_{eq} with the Excel spreadsheet. The values of K_{ism} are reported in Table 1.

The titrations of L1 with AcO^- and $H_2PO_4^-$ and L2 with $H_2PO_4^-$ present a hyperbolic curve in all the cases. The binding constants were calculated with eq 5 based on the formation of 1:1 complex. Table 1 reports the values of K obtained.

$$A_{obs} = A_H + 0.5\Delta A_\infty \times \left\{ \frac{[L]_T + [H]_T + \frac{1}{K} - \sqrt{\left([L]_T + [H]_T + \frac{1}{K}\right)2 - 4[L]_T \cdot [H]_T}}{[H]_T} \right\} \quad (5)$$

where A_{obs} is the observed absorbance, A_H is the absorbance of the free ligand, A_∞ is the maximum absorbance change induced by the presence of the given guest, $[G]_T$ is the total concentration of the guest, $[H]_T$ is the total concentration of the ligand, and K is the binding constant.

The binding constants of the systems studied are summarized in Table 1, which were about 10^3 and 10^4. The higher affinities were found with L2; this can be attributed to the lower acidity of the NH hydrogens of thiourea. In both systems, the highest constants were presented by AcO^-. However, the response of L1 to F^- is selective for color change.

FT-IR Experiments. Besides obtaining FT-IR spectra of both receptors for characterization, the spectra were compared with those of the receptor bound to guest anions F^-, AcO^-, and $H_2PO_4^-$.

Notable changes in the spectra were observed when the guest anions interacted with receptor L1 (Figure 4). In all the three cases, a wide band at 3432 cm^{-1} appeared, attributed to formation of hydrogen bonds or deprotonation of the receptor. Also, the C═O band of urea shifted from 1658 to 1710 cm^{-1}.

When L2 reacts with guest anions, also a new wide band appears at 3432 and 3460 cm^{-1}, respectively, which represents

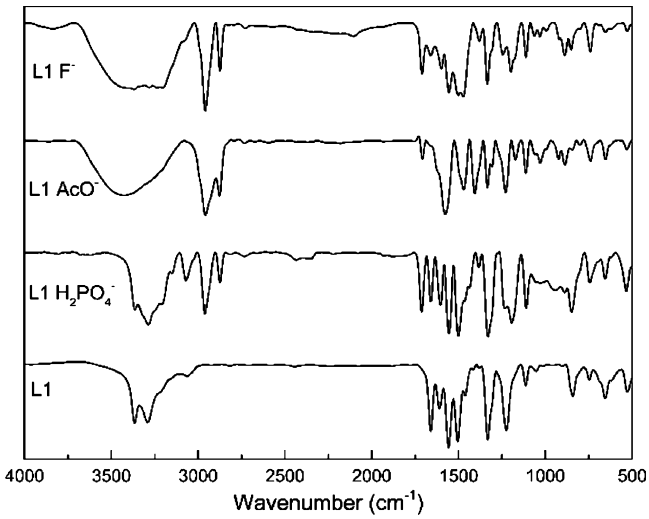

Figure 4. FT-IR spectra of L1, L1-F^-, L1-AcO^-, and L1-$H_2PO_4^-$.

the interaction between the anions and the receptor. On the other hand, there are three signals of C═S stretching in molecules with thiourea groups. In L2, these signals are at 1107, 1332, and 1597 cm^{-1}. The last signal shifts to 1670 cm^{-1} when AcO^- is present (Figure S6 of Supporting Information).

^{1}H NMR Titrations. ^{1}H NMR titrations were performed to clarify the interaction mechanism between the receptors and the guest anions.

Addition of 1 equiv of F^- to L1 (Figure 5) and L2 (Figure S8) solutions resulted in the disappearance of the OH and NH proton peaks. This spectral change indicates the occurrence of the deprotonation process in the receptors. With increasing F^- concentration, peaks corresponding to the phenolic ring protons shifted both upfield and downfield. This can be

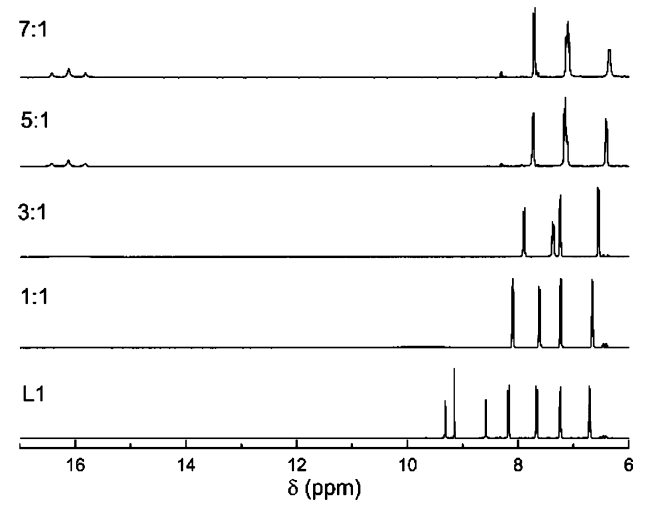

Figure 5. ^{1}H NMR titration of L1 (10 mM) by adding known quantities of TBA fluoride (1 M) in DMSO-d_6.

https://doi.org/10.1021/acsomega.0c05554
ACS Omega 2021, 6, 9381−9390

explained by two coexisting phenomena. First, by deprotonation of the hydroxy group, electron density on the phenolic group increases shielding of its protons and results in the upfield shift. Second, the interaction of the urea/thiourea group with the fluoride ion increases the aromatic ring polarity through space, resulting in the downfield shift.[22] A new triplet is shown at ∼16 ppm that can be associated to the formation of bifluoride ion (HF_2^-).[23,24]

In contrast, addition of AcO^- to L1 (Figure 6) caused a downfield displacement of NH proton peaks until equilibrium

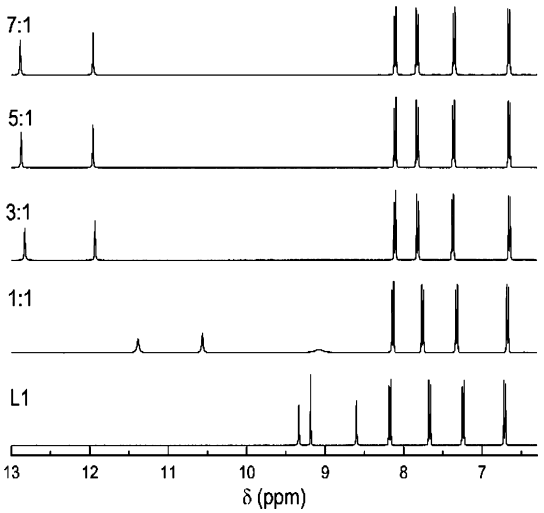

Figure 6. ^{1}H NMR titration of L1 (10 mM) adding known quantities of TBA acetate (1 M) in DMSO-d_6.

was reached. Also, the OH proton peak moved downfield but disappeared upon addition of 2 equiv of AcO^-, indicating deprotonation of this functional group. This behavior was observed also with $H_2PO_4^-$ (Figure S7). Other reported molecules with urea and thiourea groups have similar behavior that indicates the formation of parallel hydrogen bonds between the receptor and the anion.[25,26] Peaks of the aromatic ring protons did not suffer great changes, differing from protons of NH, but presented chemical shift due to the interaction.

Even under the condition that AcO^- forms hydrogen bonds with L1, in the case of L2, the addition of 1 equiv. AcO^- resulted in the deprotonation of the phenol group and of the NH groups (Figures S9 and S10) as L2 is more acidic than L1 due to the thiourea group.[27]

Computational Study. In order to understand the results obtained, theoretical studies were carried out using the density functional theory with Gaussian 09 software package; OPBE exchange−correlation function was employed along with the 6-311+G(2d,p) basis set. All chemical structures were optimized in DMSO solvent by using a polarizable continuum model (PCM). Transition wavelengths, oscillator strengths, and main contribution were summarized in Table S1, and the calculated absorption spectra are in reasonable agreement with the experimental results, in special for L2. Figure 7 presents the HOMO−LUMO and other important molecular orbitals portrayed for both receptors. The HOMOs in both receptors are mainly distributed on the aromatic ring of the phenol group side and covering their OH and NH (only one) groups, whereas the LUMOs in both receptors mainly cover the nitro group and the *o*- and *p*-positions in the aromatic ring with respect to the nitro group, although the HOMO−LUMO energy gaps are approximately equal in both receptors (5.6 eV for L1 and 5.8 eV for L2) and can be related to the first excited states as the first approximation. The results indicate that the main electronic transitions are: HOMO − 1 → LUMO and HOMO − 2 → LUMO, and HOMO → LUMO only for L1, all in singlet excited states. The HOMO − 1 and HOMO − 2 are located near to the LUMO region in both receptors, and the oscillator strength reflects a major contribution of these

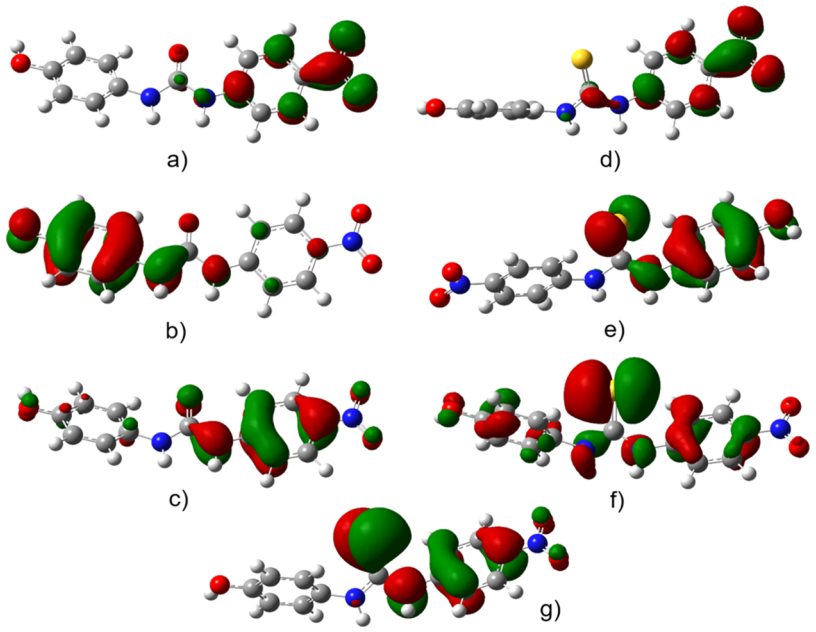

Figure 7. Main molecular orbitals in electronic transitions. For L1: (a) LUMO (−1.7 eV), (b) HOMO (−7.3 eV), (c) HOMO − 1 (−8.3 eV); for L2: (d) LUMO (−1.8 eV), (e) HOMO (−7.6 eV), (f) HOMO − 1 (−7.9 eV), and (g) HOMO − 2 (−8.0 eV). All molecular orbitals are portrayed with 0.04 au (electrons/Bohr^3) isosurface values of electron density.

https://doi.org/10.1021/acsomega.0c05554
ACS Omega 2021, 6, 9381−9390

Table 2. Bond Distances of the NH Groups of the L1 and L2 Receptors, Hydrogen Bond Distances with Each Anion, and Stretching Vibrational Frequencies of the NH Groups of L1and L2 Receptors

receptor	anion	d (anion···HN)/Å	d (H−N)/Å	ν (H−N)/cm^{-1}
L1	F^-	1.497 (H26)	1.076 (H26−N11)	2487.7 (asym. stretching)
		1.710 (H25)	1.040 (H25−N7)	3073.9 (sym. stretching)
	Cl^-	2.234 (H26)	1.021 (H26−N7)	3199.2 (asym. stretching)
		2.288 (H25)	1.027 (H25−N12)	3285.4 (sym. stretching)
	AcO^-	1.736 (O21−H30)	1.050 (H30−N11)	2854.8 (asym. stretching)
		1.766 (O24−H29)	1.045 (H29−N7)	2956.6 (sym. stretching)
	$H_2PO_4^-$	1.925 (O22−H27)	1.028 (H27−N7)	2854.8 (asym. stretching)
		1.899 (O21−H28)	1.031 (H28−N11)	2956.6 (sym. stretching)
L2	F^-	1.515 (H26)	1.073 (H26−N7)	3205.4 (asym. stretching)
		1.610 (H25)	1.054 (H25−N12)	3258.9 (sym. stretching)
	Cl^-	2.250 (H26)	1.033 (H26−N11)	3125.6 (asym. stretching)
		2.190 (H25)	1.035 (H25−N7)	3188.3 (sym. stretching)
	AcO^-	1.679 (O21−H30)	1.060 (H30−N11)	2670.8 (asym. stretching)
		1.671 (O24−H29)	1.060 (H29−N12)	2732.7 (sym. stretching)
	$H_2PO_4^-$	1.831 (O22−H27)	1.037 (H27−N7)	3068.6 (asym. stretching)
		1.822 (O21−H28)	1.038 (H28−N11)	3106.0 (sym. stretching)

molecular orbitals to the allowed transitions. Although the absorption wavelengths calculated are displaced from experimental values for L1, the calculated absorption strengths are in reasonable agreement with the experimental results. In Figures S11 and S12, UV−vis spectra calculated for L1 and L2 are presented.

In order to understand the binding mechanism of L1 and L2 to guest anions, we explored at the OPBE/6-311+G(2d,p) level the hydrogen bond distances and stretching vibrational frequencies for the interaction of the receptors with the anions, F^-, AcO^-, $H_2PO_4^-$, and Cl^- in DMSO solvent with PCM. The molecular structures, bond distances, and vibrational frequencies of the NH groups of each receptor were determined. The binding mechanisms between receptors and anions are presented in Figures S13 and S14, and the hydrogen bond distances between the anions and the NH groups are also reported in Table 2. As we can see from Figures S13 and S14, F^- approaches to a hydrogen atom at 1.497 Å for L1 and at 1.501 Å for L2. The distance of L1 is shorter than the other 1.710 Å. The NH group responsible for the shorter distance is bonded to the nitrophenyl group, and hence, this hydrogen atom is the most acidic. In addition, the NH bond distance of this group increases upon hydrogen bonding, and thereby the symmetrical and asymmetrical stretching frequencies move to lower frequencies, $\Delta\nu_{sym} = -542.5$ cm^{-1} and $\Delta\nu_{asym} = -1108$ cm^{-1} (see Table 2). The same behavior is found for interaction between L2 and F^-; in this case, the shifts of the stretching frequencies are $\Delta\nu_{sym} = -711.7$ cm^{-1} and $\Delta\nu_{asym} = -1080$ cm^{-1}. These shifts of stretching frequencies reflect much weakened NH bonds, particularly the NH bond of the most acidic hydrogen atom which is mainly involved in the normal mode of asymmetrical stretching vibration. It is noteworthy that bond distances of NH groups increase when the receptor interacts with the anion unlike when this is alone. Since the hydrogen bonds are shorter than 2 Å, they can be classified as the category of very strong, which is enough for F^- to take a proton of the NH group. In contrast to the preceding results, when Cl^- approaches to both receptors, the stretching vibrational frequencies are shifted by $\Delta\nu_{sym} = -331$ cm^{-1} and $\Delta\nu_{asym} = -396.5$ cm^{-1} for L1 and $\Delta\nu_{sym} = -442.1$ cm^{-1} and $\Delta\nu_{asym} = -377.8$ cm^{-1} for L2. This result indicates that the hydrogen bonds between Cl^- and both receptors are moderately strong, in agreement with distances larger than 2 Å, as shown in Table 2; the NH bond distance slightly increases when the receptor interacts with the anion unlike when this is alone. For interaction between AcO^- and both receptors, the stretching vibrational frequencies are shifted by $\Delta\nu_{sym} = -659.8$ cm^{-1} and $\Delta\nu_{asym} = -740.9$ cm^{-1} for L1 and $\Delta\nu_{sym} = -833.4$ cm^{-1} and $\Delta\nu_{asym} = -896.8$ cm^{-1} for L2. It should be noted that both shifts in L2 are larger than in L1, and the values are closer to $\Delta\nu_{asym}$ shifts found for interaction of F^- with L1 and L2, in consistency with the shorter hydrogen bond distances of both oxygen atoms in AcO^- that interacts with L2 compared to L1. Also, these hydrogen bonds can be classified as the category of strong, in particular for the interaction between AcO^- and L2, and the hydrogen bond distances are close to those with F^-. This behavior is similar to that of $H_2PO_4^-$. According to all these results, it is feasible to support that F^- can take a proton of the NH group (i.e., the most acidic proton) of both receptors. Similarly, AcO^- and $H_2PO_4^-$ ions, when they interact with L2, can take the two protons of the receptor in the parallel form (Figures S13 and S14).

Proposed Binding Mechanism. Using the data obtained by the different spectroscopic techniques, we propose the binding mechanisms of the receptors toward acetate, phosphate, and fluoride (Scheme 1).

As previously mentioned, receptor L1 binds to acetate and phosphate ions via hydrogen bonds. First, an approaching of the guest to the receptor occurs to cause a deprotonation of the phenol groups (Scheme 1B,C). After deprotonation, the urea group of L1 forms two parallel hydrogen bonds to two oxygen atoms of the acetate anion due to geometric complementarity.[18]

It is possible that L1 binds to fluoride with the same mechanism as L2 binds with acetate, phosphate, and fluoride anions (Scheme 1A,D,−F). Also, a deprotonation of the phenol group of the receptors takes place when guest anions approach to the receptor. Then, the anions bring about deprotonation of both NH groups of the receptors. This deprotonation depends on the acidity of the receptors due to electron-withdrawing properties of the functional groups.[18]

Synthesis and Colorimetric Detection of the Functionalized TentaGel Resins. In order to ensure practical

https://doi.org/10.1021/acsomega.0c05554
ACS Omega 2021, 6, 9381−9390

Scheme 1. Proposed Binding Mechanisms of (A) L1-F, (B) L1-AcO$^-$, (C) L1-$H_2PO_4^-$, (D) L2-F$^-$, (E) L2-AcO$^-$, and (F) L2-$H_2PO_4^-$

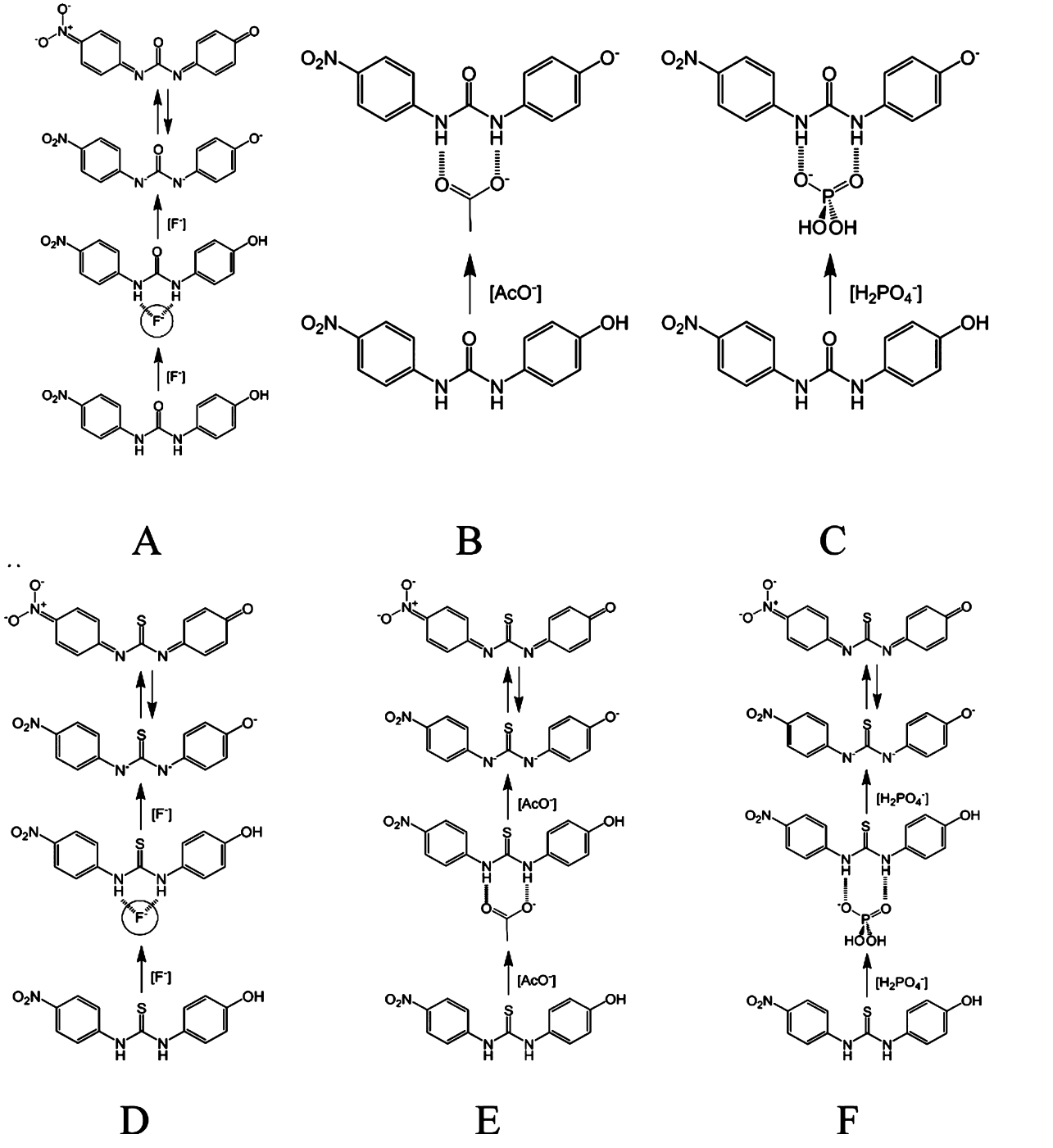

applicability of the receptors L1 and L2, they were supported on the TentaGel resin and evaluated if the sensor response observed in solution is maintained. The synthesis of two functionalized resins was achieved: one resin with receptor L1 (R1) and the other with receptor L2 (R2). There was a color change of the functionalized resins with respect to the unfunctionalized TentaGel resin from light yellow to bright yellow (Figure S15); this indicates that the receptors react with the TentaGel resin free of functional groups.[15] The characterization of the resins was carried out by FT-IR and colorimetric tests.

The detection test for the anions, which showed colorimetric changes in solution, was carried out in DMSO and water. One milligram of resin (R1 or R2) was placed in 100 μL of solvent to allow the material to swell, and subsequently, 10 μL of the salt solution in water was added. Unfortunately, R1 did not show any response by adding the anion solutions in the concentration range evaluated. In contrast, resin R2 showed a color change response when the anion solutions of AcO$^-$, $H_2PO_4^-$, or F$^-$ were added. The intensity of the color increased by increasing the anion concentration from bright yellow to red (Figure S16). Interestingly, resin R2 showed a color change response by being swelled only with water

https://doi.org/10.1021/acsomega.0c05554
ACS Omega 2021, 6, 9381−9390

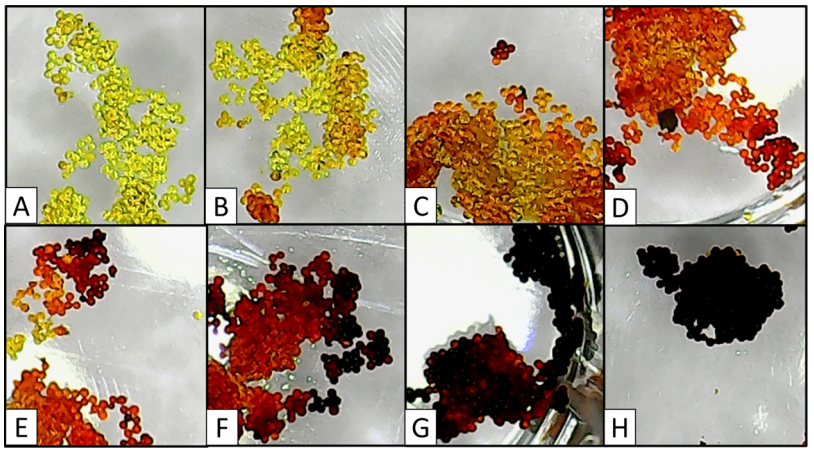

Figure 8. Sensor resin with receptor L2 (R2), and its qualitative detection of TBA fluoride in water. (A) No fluoride, (B) 0.2 mM, (C) 0.4 mM, (D) 0.6 mM, (E) 0.8 mM, (F) 1 mM, (G) 2.5 mM, and (H) 5 mM.

(Figure 8). The same color change was observed in solution, but it was necessary to increase the concentration by ten times with respect to the use in solution. The sensory response is considered outstanding since in solution, it was not possible to evaluate in a 100% aqueous medium in which the receptor was not soluble. One of the advantages of supporting to resins is that the receptors can be evaluated in other solvents, otherwise, it is not possible to do it in solution. The decrease in receptor response can be attributed to the differences in availability of the groups due to the surface effect such as the proximity to neighboring urea group or thiourea group to the polyethylene groups of PEG chain of the resins, leading to intramolecular hydrogen bonding between the urea NH protons and oxygen of the PEG.[12] In the case of R2, as the N−H are more acidic, it allows a better response. The effect of pH was also evaluated, and a color change response was found in solutions with a pH greater than 9.

CONCLUSIONS

Two simple chemosensors with urea/thiourea subunits, L1 and L2, to detect AcO^-, $H_2PO_4^-$, and F^- were synthesized and studied.

The data obtained by FT-IR, UV−vis, and ^1H NMR spectra were important for proposing the interaction mechanisms of both receptors. L1 binds to AcO^- and $H_2PO_4^-$ by forming hydrogen bonds with the urea NH groups. However, F^- deprotonates the phenol and NH groups of receptor L1. Likewise, AcO^-, $H_2PO_4^-$, and F^- deprotonate receptor L2. Color changes in the receptor solution were observed more markedly with F^-.

Both receptors were attached in TentaGel resins, and their sensing properties were qualitatively studied. No response was observed for R1, but R2 showed very high sensor response both in DMSO and water, mainly toward F^-, with a change in color from bright yellow to dark red. This event is comparable to that observed for the receptors in solution.

These results may be helpful to continue studying different strategies to create new and better anion sensors supported on solid materials for overcoming the water solubility and competition challenges present in this kind of chemosensors.

EXPERIMENTAL SECTION

General. Absorption spectra were measured at room temperature on a PerkinElmer LAMBDA 20 UV−Vis spectrometer. NMR spectra were recorded at 25 °C on a Bruker AVANCE 400 spectrometer in DMSO-d_6. FT-IR spectra were obtained on a PerkinElmer FT-IR spectrometer model Frontier. Mass spectra of electrospray ionization (ESI/MS) were obtained on 6130 Quadrupole LC/MS of Agilent Technologies. All reagents were obtained from commercial suppliers and used without further purification.

Synthesis of 1-(4-Hydroxyphenyl)-3-(4-nitrophenyl) Urea (L1). Synthesis of L1 was carried out by adding *p*-aminophenol and *p*-nitrophenylisocyanate with a 1:1 stoichiometry into a reaction flask using dry dichloromethane (DCM) as the solvent. The mixture was left in agitation for 24 h at room temperature. Afterward, the product was obtained by precipitation and it was washed using acetone. The product was dried in a vacuum oven for 5 h. 90% yield, mp of 226−227 °C, ESI/MS: 317.8.

^1H NMR (400 MHz, DMSO-d_6): 6.71 (d, J = 8.32 Hz, 2H, ArH_b), 7.24 (d, J = 8.32 Hz, 2H, ArH_c), 7.67 (d, J = 8.56 Hz, 2H, ArH_f), 8.18 (d, J = 8.56 Hz, 2H, ArH_g), 8.64 (s, 1H, $ArOH_a$), 9.20 (s, 1H, NH_d), 9.37 (s, 1H, NH_e).

^{13}C NMR (400 MHz, DMSO-d_6): 115.72, 117.68, 121.37, 125.58, 130.77, 141.17, 147.19, 152.61, 153.59.

FT-IR (KBr) cm^{-1}: 841, 1227, 1330, 1460, 1560, 1615, 1658, 3300, 3371.

Synthesis of 1-(4-Hydroxyphenyl)-3-(4-nitrophenyl)-thiourea (L2). L2 was synthesized by adding *p*-aminophenol and *p*-nitrophenylisothiocyanate with a 1:1 stoichiometry into a reaction flask using dry DCM as the solvent. The mixture was left in agitation for 24 h at room temperature. The precipitated product was washed using ACN and dried in a vacuum oven for 5 h. 90% yield, mp of 146−147 °C, ESI/MS: 307.8.

^1H NMR (400 MHz, DMSO-d_6): 6.75 (d, J = 8.12 Hz, 2H, ArH_b), 7.21 (d, J = 8.12 Hz, 2H, ArH_c), 7.82 (d, J = 8.72 Hz, 2H, ArH_f), 8.19 (d, J = 8.72 Hz, 2H, ArH_g), 9.48 (s, 1H, $ArOH_a$), 10.07 (s, 1H, NH_d), 10.22 (s, 1H, NH_e).

^{13}C NMR (400 MHz, DMSO-d_6) 115.63, 121.90, 124.75, 126.57, 130.50, 142.56, 147.00, 155.61, 179.87.

FT-IR (KBr) cm^{-1}: 850, 1260, 1330, 1560, 1609, 3300, 3272.

Synthesis of Sensor Resins. The sensor resins were synthesized by adding TentaGel HL-Br resin (loading: 0.48 mmol/g) and L1/L2 with a 1:1.1 stoichiometry into a reaction flask. The reaction was performed in basic media (triethylamine) using DMSO as the solvent. Afterward, the mixture was

https://doi.org/10.1021/acsomega.0c05554
ACS Omega 2021, 6, 9381−9390

left in agitation for 24 h at room temperature. After agitation, the resin was filtered and washed using ACN to get rid of the non-reacted receptor. The sensor resin was dried in a vacuum oven for 5 h.

Resin with L1 FT-IR cm^{-1}: 2869, 1456, 1343, 1298, 1237, 1090, 947, 841, 756, 698, 1716, 1699, 1555, 1541.

Resin with L2 FT-IR cm^{-1}: 2863, 1597, 1557, 1349, 1287, 1240, 843, 752, 695.

UV−Vis Experiments. The solutions of the receptors L1 and L2 and the guest anions were prepared in DMSO due to receptor solubility. Volume of the receptor solutions used in the UV−vis experiments was 3 mL. Absorption spectra were recorded by adding different amounts of anion solution of a known concentration into the receptor solution.

FT-IR Experiments. FT-IR spectra of the receptors within a KBr pellet were obtained. Likewise, FT-IR spectra of the guest anions were obtained. FT-IR spectra of receptors attached to TentaGel resins were obtained through ATR.

^{1}H NMR Experiments. The solution of the receptors (10 mM in DMSO-d_6) was titrated by adding known quantities of solution of TBA salts of fluoride (F^-), monobasic phosphate ($H_2PO_4^-$), and acetate (AcO^-) (1 M). The chemical shift changes of the receptors were monitored.

Computational Studies. All structure calculations were performed with the software package Gaussian 09 (G09).[28] For this work, the OPBE exchange−correlation functional[29] was employed along with the 6-311+G(2d,p) basis set. The chemical structures were optimized in DMSO solvent using a PCM.[30] Frequency analysis confirmed that all optimized structures correspond to the global minima in the potential energy surface. Furthermore, time-dependent DFT calculations as implemented in G09[31,32] with CAM-B3LYP[33,34] were carried out for evaluating the first four and five singlet and triplet excited states in both L1 and L2 receptors; this was performed taking the optimized molecular geometries and using the same basis set and DMSO solvent.

■ ASSOCIATED CONTENT

Supporting Information

The Supporting Information is available free of charge at https://pubs.acs.org/doi/10.1021/acsomega.0c05554.

^{13}C NMR spectra; mass spectra of receptors; UV-titrations of L1-$H_2PO_4^-$, L2-$H_2PO_4^-$, FT-IR of L2 and L2-F^-, L2-AcO^-, L2-$H_2PO_4^-$; NMR titrations of L1-$H_2PO_4^-$, L2-F^-, L2-AcO^-, L2-$H_2PO_4^-$; molecular structures of L1 and L2 and their complexes; UV−vis calculated for L1 and L2; photograph of resins; evaluation of R2 with F^-; and synthesis of L1, L2, R1, and R2 (PDF)

■ AUTHOR INFORMATION

Corresponding Author

Hisila Santacruz-Ortega − *Departamento de Investigación en Polímeros y Materiales, Universidad de Sonora, Hermosillo 83000, Sonora, Mexico;* orcid.org/0000-0002-7123-8791; Email: hisila.santacruz@unison.mx

Authors

Bruno Zavala-Contreras − *Departamento de Investigación en Polímeros y Materiales, Universidad de Sonora, Hermosillo 83000, Sonora, Mexico*

Angel Ulises Orozco-Valencia − *Departamento de Investigación en Polímeros y Materiales, Universidad de Sonora, Hermosillo 83000, Sonora, Mexico*

Motomichi Inoue − *Departamento de Investigación en Polímeros y Materiales, Universidad de Sonora, Hermosillo 83000, Sonora, Mexico*

Karen Ochoa Lara − *Departamento de Investigación en Polímeros y Materiales, Universidad de Sonora, Hermosillo 83000, Sonora, Mexico*

Rosa-Elena Navarro − *Departamento de Investigación en Polímeros y Materiales, Universidad de Sonora, Hermosillo 83000, Sonora, Mexico;* orcid.org/0000-0002-6744-0954

Complete contact information is available at: https://pubs.acs.org/10.1021/acsomega.0c05554

Author Contributions

The manuscript was written through contributions of all authors.

Notes

The authors declare no competing financial interest.

■ ACKNOWLEDGMENTS

This work was supported by the Consejo Nacional de Ciencia y Tecnología de México (CONACyT, Red Temática de Química Supramolecular" Proyecto 294810) and Universidad de Sonora (grant no. USO316006137). B.Z.-C. thanks CONACYT for graduate doctoral scholarship.

■ ABBREVIATIONS

L1, receptor with urea group; L2, receptor with thiourea group; R1, receptor L1 supported on TentaGel; R2, receptor L2 supported on TentaGel.

■ REFERENCES

(1) Zhou, Y.; Yoon, J. Recent Progress in Fluorescent and Colorimetric Chemosensors for Detection of Amino Acids. *Chem. Soc. Rev.* **2012**, *41*, 52−67.

(2) Kubik, S. Anion Recognition in Water. *Chem. Soc. Rev.* **2010**, *39*, 3648−3663.

(3) Kumar, G. G. V.; Kesavan, M. P.; Sivaraman, G.; Rajesh, J. Colorimetric and NIR Fluorescence Receptors for F− Ion Detection in Aqueous Condition and Its Live Cell Imaging. *Sens. Actuators, B* **2018**, *255*, 3194−3206.

(4) Hinterholzinger, F. M.; Rühle, B.; Wuttke, S.; Karaghiosoff, K.; Bein, T. Highly Sensitive and Selective Fluoride Detection in Water through Fluorophore Release from a Metal-Organic Framework. *Sci. Rep.* **2013**, *3*, 2562.

(5) Serpell, C. J.; Beer, P. D. 8.16—Anion Sensors. *Reference Module in Chemistry, Molecular Sciences and Chemical Engineering*; Atwood, J. L. B. T.-C. S. C. I. I., Ed.; Elsevier: Oxford, 2017; pp 351−385.

(6) Zhou, Y.; Zhang, J. F.; Yoon, J. Fluorescence and Colorimetric Chemosensors for Fluoride-Ion Detection. *Chem. Rev.* **2014**, *114*, 5511−5571.

(7) Gale, P. A.; Howe, E. N. W.; Wu, X. Anion Receptor Chemistry. *Chem* **2016**, *1*, 351−422.

(8) Gale, P. A.; Caltagirone, C. Fluorescent and Colorimetric Sensors for Anionic Species. *Coord. Chem. Rev.* **2018**, *354*, 2−27.

(9) Busschaert, N.; Caltagirone, C.; Van Rossom, W.; Gale, P. A. Applications of Supramolecular Anion Recognition. *Chem. Rev.* **2015**, *115*, 8038−8155.

(10) Saikia, E.; Borpuzari, M. P.; Chetia, B.; Kar, R. Experimental and Theoretical Study of Urea and Thiourea Based New Colorimetric Chemosensor for Fluoride and Acetate Ions. *Spectrochim. Acta, Part A* **2016**, *152*, 101−108.

(11) Suksai, C.; Tuntulani, T. Chromogenic Anion Sensors. *Chem. Soc. Rev.* **2003**, *32*, 192−202.
(12) Li, A.-F.; Wang, J.-H.; Wang, F.; Jiang, Y.-B. Anion Complexation and Sensing Using Modified Urea and Thiourea-Based Receptors. *Chem. Soc. Rev.* **2010**, *39*, 3729−3745.
(13) Blažek Bregović, V.; Basarić, N.; Mlinarić-Majerski, K. Anion Binding with Urea and Thiourea Derivatives. *Coord. Chem. Rev.* **2015**, *295*, 80−124.
(14) Mohanasundaram, D.; Vinoth Kumar, G. G.; Kumar, S. K.; Maddiboyina, B.; Raja, R. P.; Rajesh, J.; Sivaraman, G. Turn-on Fluorescence Sensor for Selective Detection of Fluoride Ion and Its Molecular Logic Gates Behavior. *J. Mol. Liq.* **2020**, *317*, 113913.
(15) Byrne, S.; Mullen, K. M. Urea and Thiourea Based Anion Receptors in Solution and on Polymer Supports. *Supramol. Chem.* **2018**, *30*, 196−205.
(16) Rapp, W.; Zhang, L.; W Bannwarth, E. B. Bayer in Peptides 1992. *Proceedings of the 22th European Peptide Symposium; Leiden*, 1992; p 347.
(17) Quarrell, R.; Claridge, T. D. W.; Weaver, G. W.; Lowe, G. Structure and Properties of TentaGel Resin Beads: Implications for Combinatorial Library Chemistry. *Mol. Diversity* **1996**, *1*, 223−232.
(18) Amendola, V.; Fabbrizzi, L.; Mosca, L. Anion Recognition by Hydrogen Bonding: Urea-Based Receptors. *Chem. Soc. Rev.* **2010**, *39*, 3889−3915.
(19) Fan, E.; Van Arman, S. A.; Kincaid, S.; Hamilton, A. D. Molecular Recognition: Hydrogen-Bonding Receptors That Function in Highly Competitive Solvents. *J. Am. Chem. Soc.* **1993**, *115*, 369−370.
(20) Haushalter, K. A.; Lau, J.; Roberts, J. D. An NMR Investigation of the Effect of Hydrogen Bonding on the Rates of Rotation about the C−N Bonds in Urea and Thiourea. *J. Am. Chem. Soc.* **1996**, *118*, 8891−8896.
(21) Wu, Y.; Peng, X.; Fan, J.; Gao, S.; Tian, M.; Zhao, J.; Sun, S. Fluorescence Sensing of Anions Based on Inhibition of Excited-State Intramolecular Proton Transfer. *J. Org. Chem.* **2007**, *72*, 62−70.
(22) Okudan, A.; Erdemir, S.; Kocyigit, O. 'Naked-Eye' Detection of Fluoride and Acetate Anions by Using Simple and Efficient Urea and Thiourea Based Colorimetric Sensors. *J. Mol. Struct.* **2013**, *1048*, 392−398.
(23) Amendola, V.; Bergamaschi, G.; Boiocchi, M.; Fabbrizzi, L.; Mosca, L. The Interaction of Fluoride with Fluorogenic Ureas: An ON1−OFF−ON2 Response. *J. Am. Chem. Soc.* **2013**, *135*, 6345−6355.
(24) Gómez-Vega, J.; Moreno-Corral, R. A.; Santacruz Ortega, H.; Corona-Martínez, D. O.; Höpfl, H.; Sotelo-Mundo, R. R.; Ochoa-Terán, A.; Escobar-Picos, R. E.; Ramírez-Ramírez, J. Z.; Juárez-Sánchez, O.; Lara, K. O. Anion, Cation and Ion-Pair Recognition by Bis-Urea Based Receptors Containing a Polyether Bridge. *Supramol. Chem.* **2019**, *31*, 322−335.
(25) Boyle, E. M.; Comby, S.; Molloy, J. K.; Gunnlaugsson, T. Thiourea Derived Tröger's Bases as Molecular Cleft Receptors and Colorimetric Sensors for Anions. *J. Org. Chem.* **2013**, *78*, 8312−8319.
(26) Al-Sayah, M. H.; Abdalla, A. M.; Shehab, M. K. A Dansyl-Based Optical Probe for Detection of Singly and Doubly Charged Anions. *Supramol. Chem.* **2016**, *28*, 224−230.
(27) Gómez, D. E.; Fabbrizzi, L.; Licchelli, M.; Monzani, E. Urea vs. Thiourea in Anion Recognition. *Org. Biomol. Chem.* **2005**, *3*, 1495−1500.
(28) Frisch, M. J.; Trucks, G. W.; Schlegel, H. B.; Scuseria, G. E.; Robb, M. A.; Cheeseman, J. R.; Zakrzewski, V. G.; Montgomery, J. A., Jr; Stratmann, R. E.; Burant, J. C. *Gaussian09*, Revision B.01; Gaussian. Inc.: Pittsburgh 2010.
(29) Swart, M.; Ehlers, A. W.; Lammertsma, K. Performance of the OPBE Exchange-Correlation Functional. *Mol. Phys.* **2004**, *102*, 2467−2474.
(30) Cossi, M.; Barone, V.; Cammi, R.; Tomasi, J. Ab Initio Study of Solvated Molecules: A New Implementation of the Polarizable Continuum Model. *Chem. Phys. Lett.* **1996**, *255*, 327−335.
(31) Bauernschmitt, R.; Ahlrichs, R. Treatment of Electronic Excitations within the Adiabatic Approximation of Time Dependent Density Functional Theory. *Chem. Phys. Lett.* **1996**, *256*, 454−464.
(32) Stratmann, R. E.; Scuseria, G. E.; Frisch, M. J. An Efficient Implementation of Time-Dependent Density-Functional Theory for the Calculation of Excitation Energies of Large Molecules. *J. Chem. Phys.* **1998**, *109*, 8218−8224.
(33) Yanai, T.; Tew, D. P.; Handy, N. C. A New Hybrid Exchange−Correlation Functional Using the Coulomb-Attenuating Method (CAM-B3LYP). *Chem. Phys. Lett.* **2004**, *393*, 51−57.
(34) Peach, M. J. G.; Benfield, P.; Helgaker, T.; Tozer, D. J. Excitation Energies in Density Functional Theory: An Evaluation and a Diagnostic Test. *J. Chem. Phys.* **2008**, *128*, 044118.

https://doi.org/10.1021/acsomega.0c05554
ACS Omega 2021, 6, 9381−9390